Responsivity Robustness of Radioactivity-Irradiated Nanosensors

E. A. ANAGNOSTAKIS

Nanodevice Physics Forum; Alimos, Greece.

22 Kalamakiou Ave., GR 174 55 Alimos, Greece.

emmanagn@otenet.gr

ABSTRACT

The responsivity robustness of representative photodetector-nanointerfaces with respect to the extent to which they exhibit radiation hardness and the degree of functionally tolerable radioactivity-induced responsivity de-emphasis, against increasing cumulative radioactivity-dose, is notionally considered and modelled. Systematic experimental findings concerning commercial p-i-n photodetectors being exposed to regulated successive α-particle bombardments appear in compliance with the analysis and reveal noteworthy trends of radiation-effected optoelectronic-yield alteration.

Keywords: Responsivity Robustness, Nanosensors, Radioactivity Irradiation Radiation-Hardness, Optoelectronic Reliability, Photodetectors, Photoresponsive Nanointerfaces, Quantum Efficiency & Detection Yield.

1. Introduction

The communication-technology importance of optoelectronic semiconductor photodetectors has been being righteously discussed [1 -6], with the ambient-sensitive functionality of their nanointerface interestingly focused upon [7 -12].

Unfavourable functional alteration is, still, known to result from exposure of semiconductor optical-signal sensors to a particle-irradiation environment, as in the case of optoelectronic nanodevices carried by Space vehicles [4 – 6]. And yet, appropriate assessment of such performance-consequences may allow for the emergence of a reliability interval regarding the optoelectronic responsivity of the photodetector, despite its ambient-fatigue, like its radioactivity-induced photoresponse de-emphasis, in particular.

The non-ionising energy loss of the incoming bombarmsnt particle has been monitored, for example, for GaAs and Si devices as leading to displacement damage [13]. Such lattice disruptions are believed to invoke deep-level defect-states modifying the electrical properties of the device active material and even onsetting relaxation-like and semi-insulating behaviour [14].

In the present research, the optoelectronic reliability of representative photodetector nanointerfaces with respect to the extent to which they exhibit radiation-hardness and the degree of functionally tolerable radioactivity-induced responsivity de-emphasis, against increasing cumulative radioactivity-dose, is notionally considered and modeled. Systematic experimental findings concerning commercial p-i-n photodetectors being exposed to regulated successive α-particle bombardments appear in compliance with the analysis and reveal noteworthy trends of radiation-effected optoelectronic-yield alteration.

2. Modelling Scheme

Choosing to be monitoring the optoelectronic reliability of the photodetector nanointerface ultimately through the device detection yield Y, we employ as its exact definition in this study the number of photogenerated charge carriers per incident illumination photon. Thus, it may be expressed as the ratio of the time rate of creation of flowing photocarriers (1/e)I (with e being the elementary electron-charge and I the detection photocurrent responding to the illumination beam impinging upon the photodiode under study) over the temporal rhythm of incidence of illumination photons AΦ (with A being the exposed photodiode-surface area and Φ the illuminating-beam photonic flux (photons/(cm^2 s))):

$$Y = (1/e)\, I/(A\Phi) . \quad (1)$$

On the other hand, the number (1/e)I of charge carriers photogenerated per unit time is given by that part of the number AΦ of illumination photons striking the exposed nanodevice per temporal unit which having escaped reflection at the illuminated surface (by a probability of (1-R), R being the reflectivity of the exposed-surface semiconductor at the specific illumination wavelength) inhabit mainly [15] the photodiode depletion-zone (by a cumulative occupation probability of [1 – exp(-αW)] –with α being the depletion-zone material absorption-coefficient for the specific illumination-wavelengrh and W the depletion-zone width valid for the value of reverse bias applied to the sensor under testing– , deriving as the difference between probability of photonic entrance into and probability of photonic exit from the depletion-zone extension –under the assumption of shallow depletion-zone, materialising for the technologically conventional photodetectors, like the commercial p-i-n photodiodes) and, furthermore, succeed (by a quantum efficiency of F corresponding to the specific illumination-wavelength) in being absorbed within the depletion zone, ultimately energetically liberating initially bound (in the semiconductor valence-band or at impurity or lattice-defect trap-levels) charge carriers:

$$(1/e)I=F\,[1 – \exp(-\alpha W)]\,(1-R)\,A\Phi. \quad (2)$$

It is, then, obvious that the photodetector nanointerface detection yield Y, as defined by (1), is expressible, by virtue of (2), as

$$Y = F\,[1 - \exp(-\alpha W)]\,(1-R)\ , \qquad (3)$$

which describes the detection-yield dependence upon chosen illumination-wavelength λ (through the λ-related quantities F, α, and R) and applied reverse bias V (through the phodetector diodic depletion-region width W).

A noteworthy prediction, then, regarding the radiation-hardness optoelectronic reliability of the photodetector nanointerface, as exemplified by its detection yield behaviour and sustainability, is that it would be essentially effected upon by the radioactivity dose δ influencing chiefly its (internal) quantum efficiency F (potentially codified, thus, as F(λ ; δ)), with the non-excluded possibility that, for each cumulative radioactivity-particle intaking, transcending a critical photonic flux of illumination could –through some "photonic-congestion state"– adequately liberate the detection yield from radioactive-radiation impediments.

The experimentally measured, now, conductivity current through the illuminated reverse-biased diodic phosensors comprises the optoelectronic response photocurrent I and the dark saturation - recombination current (saturation of the dark reverse current having been reached at the sufficiently high reverse bias regularly applied), both flowing in the reverse sense with respect to a forward-biased diodic photodetector's dark conduction situation.

As, then, is well known [16 – 18], the dark saturation – recombination diodic current is at a given absolute sensor- ambient temperature determined by the dark depletion-zone built-in voltage value, indicatively measuring for commercial Si p-i-n photodiodes below 200 - 300 nA against registered total conductivity-current values of units or tens of a μA through wide-range and high-level photonic fluxes. These facts render the directly measured overall conductivity-current permeating the photodetector nanointerface adequately approaching the net optoelectronic detection photocurrent I.

3. Experimental

The experimental configuration comprises the infrared (IR) LASER-beam emitter unit, an optical fiber waveguide, and the photodetector nanodevice part: Double-heterojunction AlGaAs IR- LASER diodes emitting in the 0.78 μm band are launched into the front end of a 1 m long. 3 mm in diameter, single-mode, Eska high-performance plastic optical fiber connected at its rear end to (preferentially up to this stage but not exclusively) commercially conventional, narrow receiving-angle, linear response, fast switching-time, Si p-i-n photodiodes exhibiting peak responsivity for incoming wavelengths between 0.75 and 1.00 μm.

Each double-heterostructure AlGaAs IR-LASER diode is controlled through a special, high-fidelity, current-source sustaining up to 54 mA of injection current. The optical power at the output port of the Eska fiber waveguide is exactly measured at each LASER diode injection-current level utilised by a Melles Griot, 4-digit, universal optical-power metre bearing a 10-mm-aperture Si-detector head. These optical power P measurements along with each illuminated Si p-i-n photodiode's area A lead to the respective energetic intensity $\Theta = P/A$ ($\mu W/cm^2$) values, which –through the straightforward relation $\Theta = h\,(c/\lambda)\,\Phi$,

with h being Planck's action constant and c being the universal constant of the speed of light,– furnish the photonic-flux Φ (photons/(cm^2 s)) data as witnessed by the photodetector nanodevice investigated each time, for the successive LASER-diode injection-current levels employed.

The optoelectronic response of the diodic photodetector studied per experiment whilst sensing the incident IR signal is –on the other hand– monitored at each experimental step in terms of the photocurrent I flowing through its nanointerface. For the series of optoelectronic-reliability experiments (performed at room temperature) concerning Si p-i-n photodetectors in particular and reported here, the order of magnitude of the impingent IR photonic flux Φ ranges from 4.6 x 10^{14} to 8.0 x 10^{15} photons/(cm^2 s), whereas the resulting detection-photocurrent I permeating the Si photodiodes varies from, around, 2 to 70 μA.

For each Si p-i-n IR photodetector nanointerface studied, the optoelectronic- response I-Φ characteristic curve is experimentally traced both prior to and after exposure to some decided cumulative radioactive α-particle dose δ (α-particles/cm^2) materialising through the bombarding of the photodetector at a constant α-particle-flux (α-particles/(cm^2 s)) for a prederemined time-interval.

The radioactive α-particle source utilised for the experiments described here is of ^{241}Am nuclide with a 2.87 mm face-diameter and a mean emitted α-particle energy-value of approximately 5 MeV. Care is taken that the ^{241}Am source is properly situated in almost direct contact to each exposed photodetector nanodevice for the time period desired. The exact cumulative α-particle dose to which the photodetector has been, thus, exposed is evaluated by consideration of this time interval along with the accurate α-particle flux at the site of the exposed photodiode, measured by a Leybold Heraeus Geiger – Muller counter.

The basic processing of the experimental (plausibly singly or piece-wise linear) I-Φ characteristics for any photosensor considered provides the absolute value(s) (in photogenerated flowing charge-carriers per incident visible or IR illumination-photon) of the nanodevice's detection yield Y, which in accordance with its notion and definition (1) may be obtained through the photodetector optoelectronic-response- curve slope (ΔI / ΔΦ) –calculated by a least-squares fitting– as

$$Y = [1 / (eA)] (\Delta I / \Delta \Phi) \quad . \qquad (4)$$

4. Radiation-Hardness Optoelectronic Reliability Assessment

Detailed investigations during the series of experiments have, with respect to the set of commercial encapsulated Si p-i-n photodetectors and α-particle ^{241}Am- source, traced a cumulative-dose threshold δ_0 of around, 4.2 x 10^9 α-particles/cm^2 necessary to surpass for clearly measurable radioactivity-induced performance-effects, interestingly comparably to relevant findings referring to observable particle-irradiation-produced operation-modifications in AlGAs / GaAs quantum-well IR-photodetectors [19].

Fundamental features of our systematic experimental correlation between magnitude of radioactivity-

induced performance alteration of photodetector nanointerfaces and cumulative particle-irradiation-dose intaken include the following (traceable also in representative Fig.1), registered for Si Photodiodes exposed as above:

1. Overall attenuation of the detection photocurrent I for each photonic flux Φ impinging upon the photodetector's illuminated area by a factor dropping to, about, one fifth its low-flux-regime value upon proceeding (in almost the middle of the employed flux-range [4.6×10^{14} to 8.0×10^{15}] photons/(cm^2 s)) to the high-flux region. The relative magnitude of the detection photocurrent after-exposure attenuation factors appears uniform for the different α-particle cumulative exposure-dose-levels employed (up to about $\Delta = 3.2 \times 10^{12}$ α-particles/cm^2 , wherefrom extinction-like effects seem to be setting on), though – expectedly– their absolute values are connected with the respective total radioactivity-dose for each experimentally traced I – Φ characteristic curve.

2. Splitting of the single pre-exposure optoelectronic-response linearity into two distinct consecutive after-exposure linearity-regimes of different slope (embodying the differing detection yield), stemming away from a clearly defined kink observed, uniformly for any tested cumulative particle-irradiation-dose|) at an incoming-photonic-flux level of $\Phi^* = 5 \times 10^{15}$ photons/(cm^2 s), in about the middle of the employed photonic-flux range. It is noteworthy that the high-photonic-flux after-exposure linearity-regime extends with a slope (detection yield) essentially equal to the one marking the single pre-exposure I – Φ linearity, for any α-particle cumulative exposure-dose δ surpassing the relevant threshold δ_0 and up to the "extinction demarcation" Δ.

3. Optoelectronic response dynamic stability, as manifested by the inverse of the relaxation-time

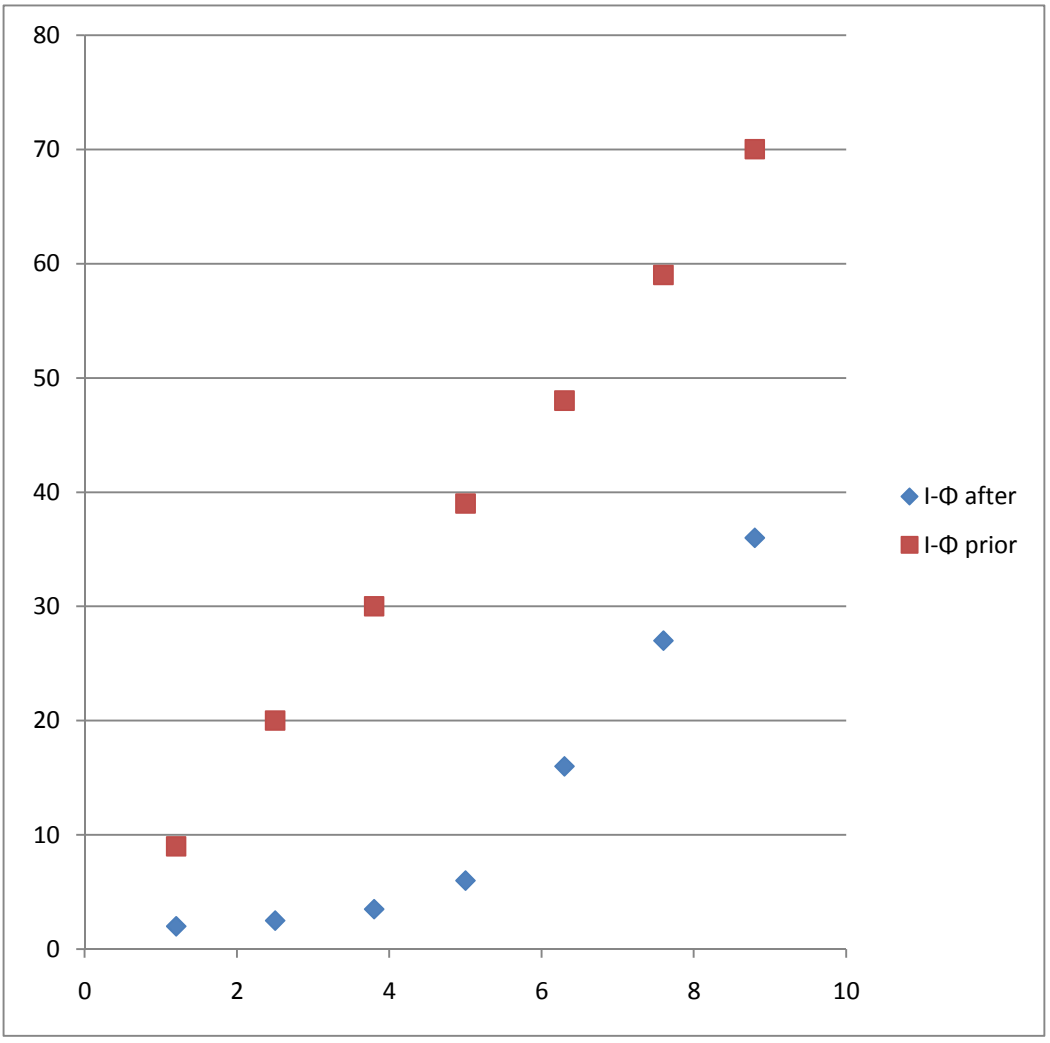

Figure 1: Representative Si p-i-n photodetector optoelectronic-response I-Φ experimental characteristic (I in μA, Φ in x10^{15} photons.(cm^2 s)) monitored prior to (upper marks) and after (lower marks) the photodiode's exposure to a cumulative α-particle dose of 3.8 x 10^{10} α-particles/cm^2 , well above the pertinent threshold.

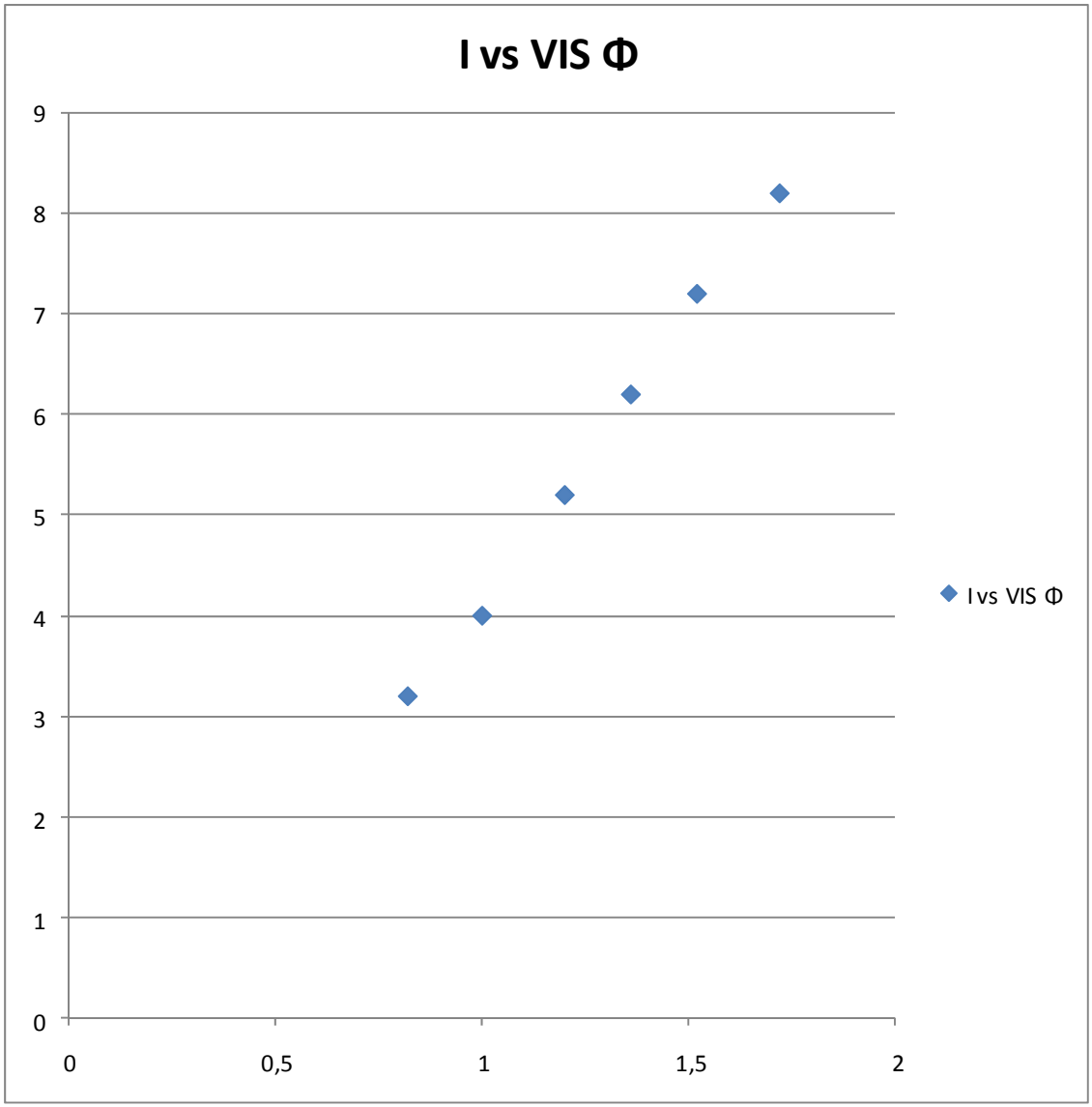

Figure 2: Experimental I – Φ characteristic of detection photocurrent I (in μA) versus incident visible at λ=650 nm photonic flux Φ (in x10^{15} photons/(cm^2 s)) for the previous (Fig.1) representative commercially conventional encapsulated Si p-i-n photodetector.

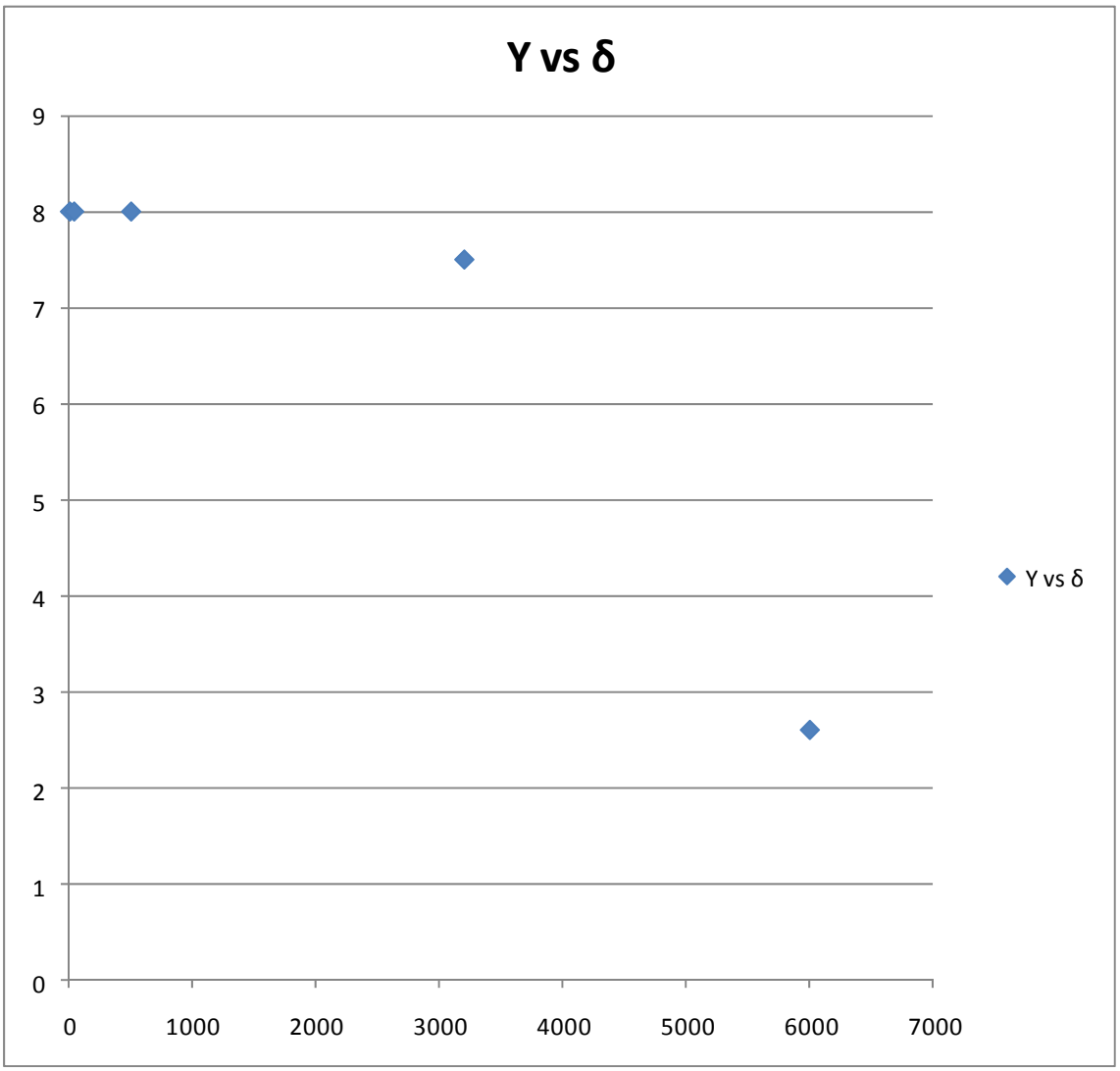

Figure 3: Evolution of the detection yield Y (given in equivalent values of the I – Φ characteristic-curve slope (ΔI / ΔΦ) in μA / (10^{15} photons/(cm^2 s))), concerning the optoelectronic response of the previous (Figs. 1 & 2) photodetector class to the applied IR illumination photonic fluxes Φ transcending the "photonic-congestion state" ignition-point Φ*= 5 x 10^{15} photons/(cm^2 s), against some of the employed values (in x 10^9 α-particles/cm^2) for the cumulative particle-irradiation dose δ increasing from radioactivity-consequence threshold δ_0 of, around, 4.2 x 10^9 α-particles/cm^2 to beyond the "extinction demarcation" Δ = 3.2 x 10^{12} α-particles/cm^2 .

preceding the fully reliable reading of the detection-photocurrent I values, degraded by almost a factor of 2.

Fig,2, concerning the optoelectronic response of the same class of photodetector nanointerfasces now illuminated by visual (VIS) at λ=650 nm photonic fluxes –provided by GaAsP LEDs controlled through another type of current source sustaining up to 200 μA of injection current intensity– , allows a comparison of the same optical signal sensor's responsivities to customary IR and VIS illumination: The respective optoelectronic-yield Y value is straightforwardly deduced to be approximately 21 photogenerated flowing charge carriers per incident infrared photon and 14 photogenerated flowing charge carriers per incident visible photon, at a comparative ratio of 3/2.

On the other hand, Fig.3 traces the evolution of the detection yield Y, concerning the optoelectronic response of the previous (Figs. 1 & 2) photodetector class to the applied IR illumination photonic fluxes Φ transcending the "photonic-congestion state" ignition-point $\Phi^* = 5 \times 10^{15}$ photons/(cm^2 s), against cumulative particle-irradiation dose δ increasing from radioactivity-consequence threshold δ_0 of, around, 4.2×10^9 α-particles/cm^2 to beyond the "extinction demarcation" $\Delta = 3.2 \times 10^{12}$ α-particles/cm^2 .

The above prime characteristics of the after-exposure optoelectronic performance of tested photodetector nanointerfaces appear understandably consistent with the adequately established observation of other researchers that particle-bombardment-invoked lattice-displacement damage results in degradation of carrier mobility and lifetime, causing a decrease in the device's optoelectronic dark-current and responsivity [20 , 21]. And yet, novel trends and invariants are herewith plausibly revealed.

5. Conclusions

In conclusion, evidence of the character of radioactivity-induced optoelectronic-performance alteration of contemporary photodetector nanointerfaces is obtained and, as regards the sample class of commercial encapsulated Si p-i-n IR photodetectors exposed to α-particle bombarding, is outlined, conducive to reliable predictions for pertinent device-functioning either in a Space-application environment or as intended radioactivity-sensors and counters.

Notably, the optoelectronic reliability (as codified by the detection yield) of photodetector nanodevices appears rather immune to radiation hardship, provided that the cumulative particle-irradiation-dose intaken does not exceed a pertinent "extinction demarcation" and that the illuminating photonic-flux transcends the "photonic-congestion state" ignition-point.

References

[1] E. A. Anagnostakis, Appl. Phys. A **54 (**1992), 68.

[2] E. A. Anagnostakis, Phys. Rev. B **46** (1992), 7593.

[3] E. A. Anagnostakis, J. Non-Cryst. Sol. **354** (2008), 4233.

[4] Y. Z. Chiou, Semicond. Sci. Technol. **24** (2009), 055004.

[5] S. W. Zeng, B. P. Zhang, J. W. Sun, J. F. Cai, C. Chen, and J. Z. Yu, Semicond. Sci. Technol. **24** (2009), 055009.

[6] D. Pons and J. C. Bourgoin, J. Phys. C: Solid State Phys. **18** (1985), 3839.

[7] D. C. Herbert, Semicond. Sci. Technol. **8** (1993), 1993.

[8] D. C. Herbert, Compel **11** (1992), 413.

[9] R. Van Overstraeten and H. De Man, Solid State Electron. **13** (1970), 583.

[10] P. H. Wilson, M. Lamm, H. C. Liu, Jianmeng Li, M. Buchanan, Z. R. Wasilewski, J. G. Simmons, and W. J. Schaff, Semicond. Sci. Technol. **8** (1993), 2010.

[11] E. Rosencher, B. Vinter, and B. F. Levine (Editors), *Intersubband Transitions in Quantum Wells* (Plenum, New York, 1992).

[12] B. F. Levine, A. Zussman, S. D. Gunapala, M. T. Ason, J. M. Kuo, and W. S. Hobson, J. Appl. Phys. **72** (1992), 4429.

[13] G. P. Summers, E. A. Burke, P. Shapiro, S. R. Messernger, and R. J. Walters, IEEE Trans. Nucl. Sci. **40** (1993), 1373.

[14] M. McPherson, B. K. Jones, and T. Sloan, Semicond. Sci. Technol. **12** (1997), 1187.

[15] D. Wood, *Optoelectronic Semiconductor Devices* (Prentice Hall International Ltd., London, 1994), Chapt. 6.

[16] S. M. Sze, *Physics of Semiconductor Devices* (Wiley – Interscience Ltd., New York, 1969), Chapt. 3.

[17] E. A. Anagnostakis, Phys. Stat. Sol. A **127** (1991), 153.

[18] E. A. Anagnostakis, Phys. Stat. Sol. B **172** (1992), K61.

[19] L. Li, H. C. Liu, P. H. Wilson, M. Buchanan, and S. M. Khanna, Semicond. Sci. Technol. **12** (1997), 947.

[20] H. Gamlouch, M. Aubin, C. Carlone, and S. M. Khanna, J. Appl. Phys. **74** (1993), 4357.

[21] A. Jorio, M. Parenteau, M. Aubin, C. Carlone, S. M. Khanna, and J. W. Jr. Gerdes, IEEE Trans. Nucl. Sci. **41** (1994), 1937.